

File ID uvapub:2030
Filename 21629y.pdf
Version unknown

SOURCE (OR PART OF THE FOLLOWING SOURCE):

Type article
Title Strong effects of photonic band structures on the diffraction of colloidal
 crystals
Author(s) W.L. Vos, R. Sprik, A. van Blaaderen, A. Imhof, A. Lagendijk, G.H. Wegdam
Faculty FNWI: Van der Waals-Zeeman Institute (WZI)
Year 1996

FULL BIBLIOGRAPHIC DETAILS:

<http://hdl.handle.net/11245/1.128414>

Copyright

It is not permitted to download or to forward/distribute the text or part of it without the consent of the author(s) and/or copyright holder(s), other than for strictly personal, individual use, unless the work is under an open content licence (like Creative Commons).

Strong effects of photonic band structures on the diffraction of colloidal crystals

Willem L. Vos and Rudolf Sprik

van der Waals–Zeeman Instituut, Universiteit van Amsterdam, 1018 XE Amsterdam, The Netherlands

Alfons van Blaaderen

*van 't Hoff Laboratorium, Universiteit van Utrecht, 3584 CH Utrecht, The Netherlands
and FOM–Institute for Atomic and Molecular Physics, 1098 SJ Amsterdam, The Netherlands*

Arnout Imhof

van 't Hoff Laboratorium, Universiteit van Utrecht, 3584 CH Utrecht, The Netherlands

Ad Lagendijk

*van der Waals–Zeeman Instituut, Universiteit van Amsterdam, 1018 XE Amsterdam, The Netherlands
and FOM–Institute for Atomic and Molecular Physics, 1098 SJ Amsterdam, The Netherlands*

Gerard H. Wegdam

van der Waals–Zeeman Instituut, Universiteit van Amsterdam, 1018 XE Amsterdam, The Netherlands

(Received 13 February 1996)

The influence of photonic band structures on optical diffraction has been studied with colloidal crystals with large refractive index ratios up to 1.45 and polarizabilities per volume as large as 0.6. It is found that the apparent Bragg spacings are strongly dependent on the wavelength of light. The dynamical diffraction theory that correctly describes weak photonic effects encountered in x-ray diffraction also breaks down. Two simple models are presented that give a much better description of the diffraction of photonic crystals. [S0163-1829(96)06523-X]

I. INTRODUCTION

The interest in photonic band structures and optical band gaps is increasing, driven by exciting prospects such as inhibition of spontaneous emission or localization of light.^{1–6} Photonic band structures occur if light travels through a three-dimensional dielectric structure with a refractive index that varies periodically on length scales comparable to the wavelength, and are analogous to electronic band structures in atomic crystals. If the refractive index ratio is larger than 1.9 and the polarizability α per “atomic” volume v (times 4π) becomes about 0.5, one can even make complete photonic band gaps^{1,2} in suitable crystal structures.³ Photonic band structures (see Fig. 1) and complete band gaps have first been observed in microwave transmission experiments by Yablonovitch Gmitter, and Leung.³ The crystals used were made by drilling arrays of holes in dielectric materials.³ To our knowledge, the shortest wavelength at which a band gap has been reported to date is $\lambda \sim 500 \mu\text{m}$ in a crystal made by stacking dielectric rods.⁶ Scaling down such structures to dimensions compatible with optical wavelengths ($\lambda \sim 500 \text{ nm}$) and consisting of many unit cells is a great challenge. An interesting alternative is the use of colloidal suspensions,⁷ because they can spontaneously organize into large crystals with lattice parameters on the order of optical length scales.⁸

Colloidal suspensions are particles with radii r between roughly 1 and 1000 nm that are suspended in liquids or gases.⁹ It is possible to synthesize particles with sizes uniform to within a few percent, which can spontaneously nucleate crystals at sufficiently high density (depending on

the charges in the system).⁸ If the lattice parameter a is of the order of optical wavelengths, crystal reflections can be visually observed as a beautiful iridescence.⁸ Optical diffraction has been applied to identify various crystal structures in systems with low refractive index contrasts or low densities ($4\pi\alpha/v < 0.05$).^{8,10–12} Optical photonic experiments have already been done on similar weakly photonic crystals.^{13–16} These demonstrate the use of colloidal crystals to applications in photonics.

In this paper, we present a study of colloidal crystals with refractive index ratios up to 1.45 and “photonic strengths” ($4\pi\alpha/v$) up to 0.6. The experiments are a significant advance towards the use of these systems in the strongly photonic regime. Diffraction experiments have been done to investigate both the optical band structures and the crystal structure. With increasing photonic strength, the band structures result in apparent Bragg spacings that strongly depend on the wavelength. Even the dynamical diffraction theory,¹⁷ which is well known in x-ray diffraction (where $4\pi\alpha/v \sim 10^{-4}$), fails to describe the observations. We present two simple models that give physically more reliable results for the lattice spacings of strongly scattering photonic crystals: first by combining Bragg’s law with linear bands using an averaged refractive index, and second using periodically stratified dielectric media.¹⁸ A preliminary account of this work has appeared in Ref. 19.

Crystal reflections are observed in diffraction experiments if the diffraction angle 2θ between the incoming and outgoing wave vectors \mathbf{k}_{in} and \mathbf{k}_{out} yields a difference vector equal to a reciprocal lattice vector \mathbf{G}_{hkl} : $\mathbf{k}_{\text{out}} - \mathbf{k}_{\text{in}} = \mathbf{G}_{hkl}$, with

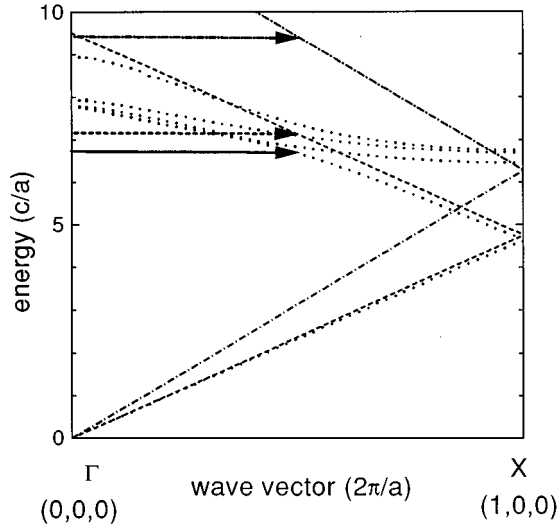


FIG. 1. Band structures calculated with the method of Leung (Refs. 3 and 5) for the 100 (X) direction of an fcc crystal with 74 vol % spheres (dots). For a complementary theoretical method, see Ref. 28. Spheres with index $n_{\text{sph}}=1.45$ and medium with $n_{\text{med}}=1.0$ were taken, corresponding to $\Psi=0.6$. For clarity, only lower bands have been plotted. The incoming wave vectors $\mathbf{k}_{\text{in}} \parallel 100$ taking part in the diffraction by a reciprocal lattice vector \mathbf{G}_{hkl} with $hkl=111$ have been indicated. The solid arrow at $E=6.7$ is \mathbf{k}_{in} corresponding to the full photonic bandstructure. The dashed arrow at $E=7.2$ is \mathbf{k}_{in} corresponding to the linear bands with a slope that is inversely proportional to the average refractive index n_{cryst} at $|\mathbf{k}|=0$ (dashed lines). The dashed-dotted arrow at $E=9.4$ is \mathbf{k}_{in} corresponding to the Bragg law: linear bands with a slope that is inversely proportional to the refractive index of the medium n_{med} (dashed-dotted lines).

hkl the Miller indices.²⁰ The length of the wave vector inside the crystal is $|\mathbf{k}|=(2\pi n)/\lambda$, with n the refractive index of the crystal, λ the wavelength of light in vacuum, and the length of \mathbf{G}_{hkl} is $|\mathbf{G}_{hkl}|=2\pi/d_{hkl}$, with d_{hkl} the lattice spacing of the hkl crystal planes. In diffraction experiments on photonic crystals as a function of the wavelength λ , asymptotic limits for small d_{hkl}/λ yield information on the reciprocal lattice vectors \mathbf{G}_{hkl} and the crystal structure, whereas information about the dispersion curves is contained in the wave vectors \mathbf{k}_{in} and \mathbf{k}_{out} . For weak photonic strengths, the dispersion relation between the energy E and the wave vectors is linear: $E=c|\mathbf{k}|$, and we obtain the well-known Bragg law: $d_{\text{Bragg}}=\lambda/(2n_{\text{med}}\sin\theta)$, with n_{med} the refractive index of the medium in which the particles are suspended (see Fig. 1). With increasing photonic strengths, the dispersion curves become nonlinear, and stop gaps appear at the edges of the Brillouin zone. The diffraction condition is modified compared to the Bragg case and fulfilled at a lower energy (Fig. 1). In the limit of weak photonic strengths, improvements on the Bragg law can be calculated exactly with the dynamical diffraction theory,¹⁷ which is well known for x-ray diffraction. The relation between the lattice spacing d_{dyn} and the diffraction angle is, for specular reflections,

$$d_{\text{dyn}}=\frac{\lambda}{2n_{\text{med}}\sin\theta}\left(1+\frac{\Psi}{2\sin^2\theta}\right)^{1/2}, \quad \Psi=3\phi\frac{m^2-1}{m^2+2}, \quad (1)$$

where ϕ is the volume fraction of colloidal spheres, m is the ratio of the refractive index of the spheres and the medium, $m=n_{\text{sph}}/n_{\text{med}}$, and Ψ is a photonic strength parameter that measures the interaction strength of the light and photonic crystal. It can be rewritten as

$$\Psi=4\pi\frac{\alpha}{v}, \quad (2)$$

which can be physically interpreted as the ratio between the ‘‘optical’’ volume and the actual volume of the scattering particles. The effects of photonic strength become more apparent for smaller θ or larger d_{hkl}/λ , which corresponds to higher bands in Fig. 1. An increase of Ψ results in an increase of the diffraction angle 2θ .

II. EXPERIMENT

Crystals were grown from silica spheres ($n_{\text{sph}}=1.45$) with radii between 108 and 525 nm, suspended in DMF (dimethylformamide), ethanol, and water ($n_{\text{med}}=1.43, 1.36$, and 1.33 , respectively). For details of the synthesis and characterization of the spheres, see Refs. 21–23. The samples crystallized after sedimentation under gravity in 400- μm -thick and 4-mm-wide glass capillaries. Crystals in air ($n_{\text{med}}=1.00$) were made from sedimented crystals by letting the suspending liquid evaporate slowly over several weeks. The samples were mounted in a cylindrical bath containing glycerine ($n=1.47$), which closely matches the refractive index of the capillaries. This bath was mounted on a rotating stage (ω circle). Because colloidal crystals often order with the close-packed planes parallel to the walls of the cell,²⁴ the diffracted intensity of these crystal planes becomes very strong and clearly visible on a screen if it coincides with the specularly reflected laser beam. Incident monochromatic light had wavelengths λ between 458 and 785 nm. Scattered radiation was detected with a photodiode, mounted on an independently rotating stage (2θ circle). The measured values of 2θ were corrected for refraction at the bath-capillary-crystal interfaces.

III. RESULTS

Representative diffraction patterns of close-packed lattice planes at $\lambda=633$ nm for samples with increasing photonic parameters, but comparable lattice parameters, are shown in (Fig. 2). Crystals with $\Psi=0.017$ reveal sharp diffraction lines near $2\theta=75^\circ$, which corresponds to a lattice spacing $d_{hkl}=380$ nm. For $\Psi=0.115$, the diffraction peak is shifted to a larger scattering angle of 80° . This is caused by an increase of Ψ and also by a decrease of the total refractive index of the system, whereas $d_{hkl}=370$ nm. For $\Psi=0.60$, the diffraction angle has moved to 97° . This is caused by the increase of Ψ , in addition by the decrease of the total refractive index of the system, and a slightly smaller $d_{hkl}=350$ nm. The diffracted signal appears to consist of several fringe-like features. These are not caused by interference in the walls of the capillary (300 μm thick), which would give a fringe period of 0.04° . Moreover, reducing Ψ of such a sample to 0.017 by reintroducing fluid in the capillary results again in a single sharp diffraction peak near $2\theta=75^\circ$, iden-

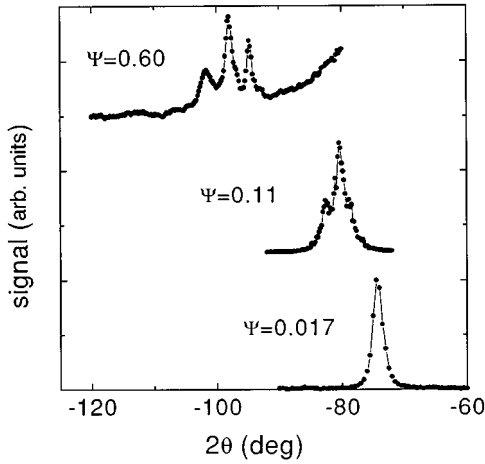


FIG. 2. Diffraction patterns of colloidal crystals. The diffraction patterns have been normalized and offset for clarity. From bottom to top: spheres with $r=211$ nm in DMF ($\Psi=0.017$), in water ($\Psi=0.11$), and in air ($\Psi=0.6$).

tical to the lower diffraction pattern in Fig. 2. Therefore, it is concluded that samples with increasing Ψ produce diffraction peaks at higher diffraction angle, which is so far consistent with the dynamical theory. We note that the volume fractions of the spheres in the crystals that are calculated from the lattice spacings and the known radii of the spheres, agree with estimates obtained from the volume fraction of the starting suspension and the ratio of the volumes of the crystal formed and the total sample.

From the measured diffraction angle 2θ , the Bragg spacing d_{Bragg} and the dynamic spacing d_{dyn} between the close-packed lattice planes are calculated and plotted in Fig. 3. For $\Psi=0.017$, Fig. 3(a) reveals that d_{Bragg} decreases slightly as a function of wavelength λ . The values of d_{dyn} are lower and nearly independent of λ , the difference with d_{Bragg} decreasing to long λ as expected. A similar result was obtained for

a dilute charged system with $\Psi=0.005$. In contrast, the results for $\Psi=0.115$ show a strong increase of d_{Bragg} of 50% in going from 785 to 458 nm [Fig. 3(b)]. This means that d_{Bragg} has become an unphysical estimate of the lattice spacing. A more reliable result is obtained with the dynamic theory, because d_{dyn} is independent of λ . At the longest wavelengths, d_{Bragg} converges to d_{dyn} as expected from Eq. (1). This confirms that long-wavelength extrapolations may be used to estimate the real lattice spacings of photonic crystals. Similar results were obtained for a sample with $\Psi=0.067$. For $\Psi=0.60$, Fig. 3(c) reveals a giant increase of d_{Bragg} with decreasing λ . For this strongly scattering sample, it appears that the dynamic theory is also not appropriate anymore, because d_{dyn} clearly decreases with decreasing λ . Furthermore, the values of d_{dyn} would imply that the colloidal spheres are strongly overlapping. With increasing wavelength, both apparent lattice spacings converge to a value expected for touching close-packed spheres (344 nm). We can exclude the possibility that the dispersive effects are caused by a smearing of the reciprocal lattice points due to mixed stacking, because smearing does not happen for close-packed lattice planes.⁸

IV. DISCUSSION

We have used two simple models that go beyond dynamical diffraction theory to describe the relation among the diffraction angle, the wavelength, and the physical properties of the crystals. The first model consists of approximating the apparent spacings d_{Bragg} and d_{dyn} of every hkl reflection with those of one-dimensional pairs of layers of dielectric material.¹⁸ One layer of each pair is assigned the refractive index n_{sph} of the colloidal spheres and the other that of the medium (n_{med}). The thickness d of each pair of layers is fixed to the expected lattice spacing d_{hkl} . The relative thickness is fixed by the relation between the volume fraction of

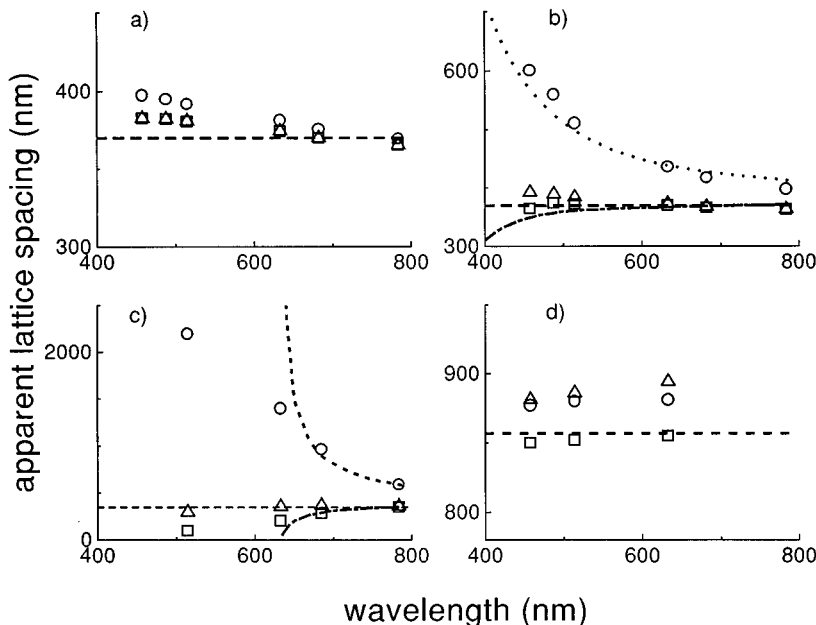


FIG. 3. Close-packed crystal spacings as a function of the wavelength of light. The long-dashed line indicates the expected spacing of the spheres, the circles are Bragg spacings, the squares are spacings calculated with the dynamic theory, and the triangles are Bragg spacings using the average index of the crystal n_{cryst} . The short-dashed curves are the Bragg spacings and the dashed-dotted curves the dynamic spacings of the periodically stratified media model. (a) spheres with $r=211$ nm in DMF ($\Psi=0.017$), (b) in H_2O ($\Psi=0.11$), (c) in air ($\Psi=0.6$), and (d) spheres with $r=525$ nm in DMF ($\Psi=0.017$).

spheres ϕ , their radius r , and d , assuming hexagonal dense packing: $\phi = (16\pi)/3[r/(d\sqrt{3})]^3$. From the calculated reflection angle, d_{Bragg} and d_{dyn} are found. In Fig. 3(b), it is seen that this gives reasonable results for $\Psi = 0.11$. In Fig. 3(c) ($\Psi = 0.60$), the results are seen to agree with the experiments at longer wavelengths. This confirms that the observed diffraction features of Fig. 2 are caused by close-packed layers of colloidal spheres. Thus, this simple model provides a reliable estimate of the crystal spacings in crystals with moderate index variations, where the dynamic theory collapses. Limitations of this model are that the shape of the calculated diffraction pattern differs from the experimental curves, and the width of the diffraction line is strongly overestimated.

In the second model, the dielectric constants of the constituent materials are combined to an average n_{cryst} by applying the Maxwell-Garnett theory²⁵ to the crystalline configuration of colloidal spheres in the surrounding medium.²⁶ This produces an average refractive index n_{cryst} that agrees well with the exact solution in the limit $|\mathbf{k}| = 0$ (Fig. 1), but at the same time washes out all crystalline features. Therefore, point scatterers are assumed to be present on the positions of the colloidal spheres to account for the diffracted light. The lattice spacings are then calculated with the Bragg law, using n_{cryst} instead of the index of the medium n_{med} . Figure 3(c) reveals that this model yields lattice spacings that agree much better with the expected values than both the Bragg or dynamic theories. Indeed Fig. 1 shows that for a dielectric crystal corresponding to Fig. 3(c), the diffraction condition is met for 10% higher energy than in the exact solution. This is in much better agreement with the exact results than the Bragg result.

In order to probe higher energies in the band structures (see Fig. 1), we have also done experiments on close-packed crystals ($\phi = 74$ vol %) of much larger spheres ($r = 525$ nm).

This corresponds to d_{hkl}/λ up to 1.9, compared to 0.8 for the crystals described above. We find that for $\Psi = 0.017$, the dynamic estimate of the lattice spacing is in excellent agreement with the value based on the 2nd and 3rd harmonic of the close-packed reflection [Fig. 3(d)], on independent experiments with confocal microscopy, and on the size of the spheres.²⁷ The Bragg law combined with the averaged refractive index n_{cryst} gives results that are about 3% higher. The deviations between these two estimates are contrasted with their excellent agreement in Fig. 3(a), and are likely caused by a greater difference between the linear bands using n_{cryst} (effective medium) and the exact bands (Fig. 1). This indicates that a photonic parameter should include the relevant energy scale. Furthermore, these results indicate why deviations from the dynamic diffraction theory have not been observed in Refs. 10–12: those experiments were done on crystals with much smaller lattice spacings, corresponding to $(d_{hkl}/\lambda) < 0.4$. Finally we note that the parameter Ψ should be improved to take into account excluded volume effects: it has the wrong limit when the volume fraction of high-index material goes to 1, in which case photonic effects are expected to go to zero again. It seems more reasonable that a photonic parameter vanishes in the limit of pure components, $\phi = 0$ or $\phi = 1$. John has suggested that photonic band gaps are optimal for $\phi = 1/(2m)$.⁷

ACKNOWLEDGMENTS

We thank Henk Lekkerkerker, Nynke Verhaegh, and David Weitz for discussions. This work was part of the research program of the Dutch Organization for Fundamental Research on Matter (FOM) and was made possible by financial support of the ‘‘Nederlandse Organisatie voor Wetenschappelijk Onderzoek’’ (NWO).

-
- ¹E. Yablonovitch, *Phys. Rev. Lett.* **58**, 2058 (1987).
²S. John, *Phys. Rev. Lett.* **58**, 2486 (1987).
³E. Yablonovitch, T. J. Gmitter, and K. M. Leung, *Phys. Rev. Lett.* **67**, 2295 (1991).
⁴*Photonic Band Gaps and Localization*, edited by C. M. Soukoulis (Plenum, New York, 1993).
⁵*Development and Applications of Materials Exhibiting Photonic Band Gaps*, edited by C. M. Bowden, J. P. Dowling, and H. O. Everitt, special issue of *J. Opt. Soc. Am. B* **10**, 280 (1993).
⁶E. Özbay, E. Michel, G. Tuttle, R. Biswas, K. M. Ho, J. Bostak, and D. M. Bloom, *Opt. Lett.* **19**, 1155 (1994).
⁷S. John, in *Photonic Band Gaps and Localization* (Ref. 4), p. 1.
⁸P. N. Pusey, in *Liquids, Freezing, and the Glass Transition*, edited by D. Levesque, J.-P. Hansen, and J. Zinn-Justin (Elsevier, Amsterdam, 1990).
⁹R. J. Hunter, *Foundations of Colloid Science* (Clarendon, Oxford, 1992).
¹⁰T. Yoshiyama, I. Sogami, and N. Ise, *Phys. Rev. Lett.* **53**, 2153 (1984).
¹¹P. A. Rundquist, P. Photinos, S. Jagannathan, and S. A. Asher, *J. Chem. Phys.* **91**, 4932 (1989).
¹²Y. Monovoukas, G. G. Fuller, and A. P. Gast, *J. Chem. Phys.* **93**, 8294 (1990).
¹³P. L. Flaugh, S. E. O'Donnell, and S. A. Asher, *Appl. Spectrosc.* **38**, 847 (1984).
¹⁴J. Martorell and N. M. Lawandy, *Phys. Rev. Lett.* **66**, 887 (1991).
¹⁵C. J. Herbert and M. S. Malcuit, *Opt. Lett.* **18**, 1783 (1992).
¹⁶I. I. Tarhan, M. P. Zinkin, and G. H. Watson, *Opt. Lett.* **20**, 1571 (1995); *Phys. Rev. Lett.* **76**, 315 (1996).
¹⁷W. H. Zachariasen, *Theory of X-ray Diffraction in Crystals* (Wiley, New York, 1945).
¹⁸M. Born and E. Wolf, *Principles of Optics* (Pergamon, Oxford, 1980).
¹⁹W. L. Vos, R. Sprik, A. Lagendijk, G. H. Wegdam, A. Imhof, and A. van Blaaderen, in *Postdeadline Digest, 1994 European Quantum Electronics Conference* (IEEE, Piscataway, 1994). Note that this paper lacks the factor of 2 in front of the $\sin^2\theta$ term. Also W. L. Vos, R. Sprik, A. Lagendijk, G. H. Wegdam, A. van Blaaderen, and A. Imhof, in *Photonic Band Gap Materials*, edited by C. M. Soukoulis (Kluwer, Dordrecht, in press).
²⁰N. Ashcroft and D. Mermin, *Solid State Physics* (Holt, Rinehart, and Winston, New York, 1976).
²¹A. van Blaaderen and A. P. M. Kentgens, *J. Non-Cryst. Solids* **149**, 161 (1992).
²²A. Imhof, A. van Blaaderen, G. Maret, J. Mellema, and J. K. G. Dhont, *J. Chem. Phys.* **100**, 2170 (1993).

²³A. van Blaaderen and A. Vrij, *Langmuir* **8**, 2921 (1992).

²⁴See, e.g., N. A. Clark, A. J. Hurd, and B. J. Ackerson, *Nature* (London) **281**, 57 (1979); C. A. Murray, W. O. Sprenger, and R. A. Wenk, *Phys. Rev. B* **42**, 688 (1990).

²⁵See, e.g., C. F. Bohren and D. R. Huffman, *Absorption and Scat-*

tering of Light by Small Particles (Wiley, New York, 1983).

²⁶S. Datta, C. T. Chan, K. M. Ho, and C. M. Soukoulis, *Phys. Rev. B* **48**, 14 936 (1993).

²⁷A. van Blaaderen and P. Wiltzius, *Science* **270**, 1177 (1995).

²⁸J. B. Pendry, *J. Mod. Opt.* **41**, 209 (1994).